Table I. Electronic Spectra of Red-Brown Fractions from Ion Exchange of Cr^{2+} + ICH_2CO_2H Reaction Products[a]

fraction				
[eluent],[b] M	vol,[c] mL	abs max, nm (ϵ,[d] M^{-1} cm^{-1})		
0.5	0–10	548 (30.4)	414.5 (69.2)	271 (2.50×10^3)
0.5	10–20	552 (27.1)	414 (58.9)	272 (1.91×10^3)
0.5	20–80	554 (25.7)	413 (50.5)	270.5 (1.52×10^3)
0.5	80–120	551 (27.3)	412 (55.3)	270.5 (1.74×10^3)
3–4	200–300	524 (48.8)	408 (74.5)	271 (2.84×10^3)

[a] The initial reaction solution contained 0.15 M Cr^{2+} and 0.105 M ICH_2CO_2H in 0.75 M $HClO_4$. [b] Eluent is $HClO_4$ in all cases. [c] Volume of fraction collected at flow rate of ~10 mL min^{-1}. [d] Extinction coefficients are based on total chromium determined by oxidation to chromate with H_2O_2. Since all were measured under the same conditions in the same cells, the relative uncertainty between values is ≤1%.

The results, summarized in Table I, give the properties of various red-brown fractions of the fraction initially eluted from X2 in 0.5 M $HClO_4$. The longest wavelength peak shifts from 548 to 554 nm for the first three fractions, while the extinction coefficients decrease in the 550- and 270-nm regions. The fourth fraction reverses this trend, and the final fraction in 3–4 M $HClO_4$ shows a substantial blue shift to 524 nm, and an increase in extinction coefficients at all absorption maxima.

The results in Table I can be explained if the red-brown band is actually a mixture of $(H_2O)_5CrCH_2CO_2H^{2+}$ and $(H_2O)_5CrO_2CCH_3^{2+}$, which are not fully separated by the rather rapid ion-exchange conditions necessary to combat the oligomerization reaction discussed above. The relative amount of $(H_2O)_5CrO_2CCH_3^{2+}$ must increase from fractions 1 through 3 to explain the changes in position of the absorption maxima and apparent extinction coefficients.[6] The fourth fraction probably contains some oligomer (e.g. $n = 1$, charge = 3+), and the final fraction in 3–4 M $HClO_4$ contains higher oligomers.

A further peculiarity of the organochromium(III) product is shown by its reaction with mercury(II). This reaction normally proceeds as[7]

$$(H_2O)_5CrCH_2R + Hg^{2+} \xrightarrow{H_2O} Cr(OH_2)_6^{3+} + HgCH_2R^+ \quad (3)$$

When a portion of the third fraction in Table I was mixed with excess $Hg(ClO_4)_2$ in 0.5 M $HClO_4$ (Hg(II):Cr(III) = 2:1), the solution quickly changed from red-brown to green, but no $Cr(OH_2)_6^{3+}$ was detected after ion-exchange separation. Only two species were separated. A blue species is easily eluted from Dowex 50W-X2 with 0.5 M $HClO_4$, and its absorption maxima, 571 and 411 nm, and extinction coefficients, 25.0 and 23.8 M^{-1} cm^{-1}, respectively, indicate that it is $(H_2O)_5CrO_2CCH_3^{2+}$.[6] This species is present as a product of the initial reaction of Cr(II) and ICH_2CO_2H. The second product eluted with 2 M $HClO_4$ is blue also with absorption maxima at 571 and 409 nm and extinction coefficients of 20.8 and 20.9 M^{-1} cm^{-1}, respectively. This second product contains 39.5% of the total chromium(III) in the original third fraction,[8] and it contains mercury as shown by reaction with Cu metal.

The original organochromium species must be formulated to explain the facts that the reaction with mercury(II) yields no $Cr(OH_2)_6^{3+}$ and that the reaction product contains both Cr(III) and Hg(II). This behavior is consistent if the original species is a chelate (I). Then the reaction proceeds according to eq 4. The electronic spectrum of II is similar to that of $(H_2O)_5CrO_2CCH_3^{2+}$, as expected. The protonated form of I seems to be required by the similarity in charge of I and $(H_2O)_5CrO_2CCH_3^{2+}$ as implied by the difficulty in separating the two species by ion-exchange chromatography. Since the spectrum of I is unchanged in 0.10 and 0.50 M $HClO_4$, it must have a K_a < 0.1 M.

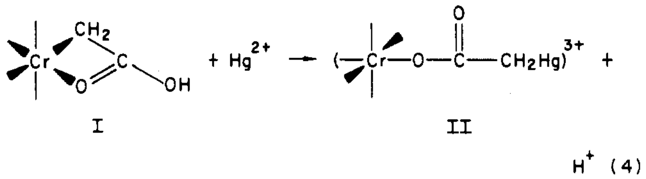

From the knowledge gained about the reactivity of the organochromium(III) species (I), it is possible to design a convenient experiment to determine the amount of $(H_2O)_5CrO_2CCH_3^{2+}$ formed from Cr^{2+} + ICH_2CO_2H. When the reaction is complete, excess $Hg(ClO_4)_2$ can be added to catalyze aquation of $(H_2O)_5CrI^{2+}$ and to convert I to II. Then the solution will contain $(H_2O)_5CrO_2CCH_3^{2+}$, $Cr(OH_2)_6^{3+}$, and $(H_2O)_5CrO_2CCH_2Hg^{3+}$, and the first species can be separated easily from the others to determine the amount formed. When 0.15 M Cr^{2+} reacts with 0.15 M ICH_2CO_2H in 0.50 M $HClO_4$, 81% of the ICH_2CO_2H reacting appears as $(H_2O)_5CrO_2CCH_3^{2+}$ in the product.

The results reported here provide a basis for reassessing the results of numerous studies[7] on the chromium(II) reduction of various organic carboxylic acids. These observations provide an important basis for predicting the prescence of oligomerization reactions and chelated species in organochromium systems.

Experimental Section

Chromium(II) perchlorate (~0.5 M in 0.10 M $HClO_4$) was prepared by reducing chromium(III) perchlorate with amalgamated zinc under argon. Sodium iodoacetate (Fisher) was used as supplied. The $Hg(ClO_4)_2$ solutions were prepared by dissolving HgO (yellow) (Anachemia) in excess perchloric acid. Low-temperature ion exchange was done in a cold room at +5 °C. The electonic spectra were recorded on a Cary 219 spectrophotometer. Standard methods of handling and analysis are described elsewhere.[2]

Acknowledgment. The authors wish to acknowledge the financial support for this research from the Natural Sciences and Engineering Research Council of Canada. P.K. wishes to thank N. Copernicus University, Torun, Poland, for granting a leave of absence to do this work.

Registry No. $Cr(ClO_4)_2$, 13931-95-8; ICH_2CO_2H, 64-69-7; $(H_2O)_5CrI^{2+}$, 18955-06-1; $Cr(OH_2)_6^{3+}$, 14873-01-9; $(H_2O)_5CrO_2CCH_3^{2+}$, 18894-45-6; $(H_2O)_5CrCH_2CO_2H^{2+}$, 52032-35-6; $(H_2O)_5CrO_2CCH_2Hg^{3+}$, 96807-98-6.

---

[8] If the 39.5% represents the amount of organochromium species in the third fraction, and 60.5% is $(H_2O)_5CrO_2CCH_3^{2+}$, then the known spectrum of the latter[6] can be used to calculate the extinction coefficients of the organochromium species at 554, 413, and 270 nm as 26, 69, and 2.5×10^3 M^{-1} cm^{-1}, respectively.

Contribution from the Departamento de Quimica Fundamental,
Universidade Federal de Pernambuco-UFPE,
50000 Recife-PE, Brazil

Theoretical Study of the Electronic Structure and Bonding in $Ni(PF_3)_4$

M. Braga

Received September 6, 1984

Although formerly subject to controversy, it is now generally considered that substituted phosphines are capable of important π-acceptor behavior.[1] However, the extent of the π bonding depends strongly on the nature of the groups attached to the phosphorus atom, particularly on the electronegativity and the size of these groups. For a long time now, chemists have realized that the ligand PF_3 is quite similar to CO[2] in both its σ-donor and π-acceptor characteristics. Experimental evidence from IR,[3]

---

[1] See, for instance: "Transition Metal Complexes of Phosphorus, Arsenic and Antimony Ligands"; McAuliffe, C.A., Ed.; Macmillan: London, 1973. McAuliffe, C. A.; Levason, W. "Phosphine, Arsine and Stibine Complexes of the Transition Elements"; Elsevier: Amsterdam, 1979. Booth, G. *Adv. Inorg. Chem. Radiochem.* **1964**, *6*, 1–69. Emsley, J.; Hall, D. "The Chemistry of Phosphorus"; Wiley: New York, 1976.

[2] Chatt, J.; Williams, A. A. *J. Chem. Soc.* **1951**, 3061–3067.

0020-1669/85/1324-2702$01.50/0 © 1985 American Chemical Society

Table I. Orbital Energies, Integrated Charge Density (in Percent of One-Electron Charge), and Orbital Characters for $Ni(PF_3)_4$

	l up to 2 on P				*l* up to 1 on P				
		charges in muffin-tin spheres				charges in muffin-tin spheres			
orbital	orbital energy, −Ry	Ni	P	F	orbital energy, −Ry	Ni	P	F	orbital character
$9a_1$	1.408	1.44	37.34	60.35	1.415	2.06	39.55	56.13	PF_3 $6a_1$
$10a_1$	1.062	4.62	16.68	59.11	1.059	7.06	21.91	50.14	PF_3 $7a_1$
$11a_1$	0.774	19.97	27.78	37.36	0.719	15.48	18.60	49.03	PF_3 $8a_1$, Ni 4s
$1a_2$	0.896	0.0	0.0	89.32	0.858	0.0	0.0	88.59	PF_3 $1a_2$
4e	1.202	0.15	22.19	74.20	1.157	0.45	24.99	72.63	PF_3 4e
5e	0.980	0.01	4.51	82.65	0.894	0.0	0.33	84.85	PF_3 5e
6e	0.933	0.38	2.23	85.39	0.874	0.06	0.09	86.68	PF_3 6e
7e	0.555	88.09	2.55	2.18	0.514	90.65	0.29	2.03	Ni 3d
8e	0.055	5.27	13.61	12.58	0.034	2.03	2.99	10.09	PF_3 7e, Ni 3d
$4t_1$	1.203	0.02	21.32	72.59	1.145	0.06	24.73	74.06	PF_3 4e
$5t_1$	0.979	0.0	4.61	83.28	0.893	0.01	0.22	85.18	PF_3 5e
$6t_1$	0.927	0.02	2.03	86.87	0.867	0.0	0.10	87.48	PF_3 6e
$7t_1$	0.901	0.0	0.04	88.58	0.861	0.0	0.01	88.20	PF_3 $1a_2$
$11t_2$	1.365	0.81	36.19	62.68	1.369	1.17	38.84	58.61	PF_3 $6a_1$
$12t_2$	1.162	0.07	20.15	74.91	1.091	0.26	22.85	74.79	PF_3 4e
$13t_2$	1.011	2.16	12.94	70.94	0.992	4.97	20.10	59.90	PF_3 $7a_1$
$14t_2$	0.970	0.55	3.95	81.21	0.904	0.21	0.10	82.89	PF_3 5e
$15t_2$	0.936	0.16	1.75	84.22	0.882	0.09	0.27	85.18	PF_3 6e
$16t_2$	0.740	35.11	32.09	24.35	0.700	26.44	24.34	37.30	PF_3 $8a_1$, Ni 3d, 4p
$17t_2$[a]	0.481	57.09	13.39	7.23	0.451	63.81	7.62	7.87	Ni 3d, 4p, PF_3 $8a_1$, 7e
$18t_2$	0.106	9.83	22.29	8.32	0.103	7.32	12.57	7.53	PF_3 7e, Ni 3d
$19t_2$	0.015	2.68	22.64	17.85					PF_3 $9a_1$

[a] Highest occupied MO (HOMO).

photoelectron,[4,5] and ion cyclotron resonance[6] spectroscopies strongly supports this view. It was commonly thought that the empty phosphorus $3d_\pi$ orbitals were responsible for the phosphorus π-acceptor capability;[1,7] i.e., the lowest unoccupied molecular orbital (MO) of π symmetry in substituted phosphines was considered to be largely localized on the phosphorus and to have substantial 3d character. However, recent theoretical studies using the SCF–Xα[8] and ab initio[9] calculations have indicated a completely different situation. The first virtual (unoccupied) level of π type is essentially of phosphorus 3p character with a small 3d component. Some early calculations on transition-metal complexes with phosphine have also questioned the existence of a phosphorus $3d_\pi$ acceptor orbital.[10,11]

The multiple-scattering–Xα (MS–Xα) method[12] has been successfully applied to study the electronic structure of transition-metal complexes containing π-acceptor ligands such as the transition-metal carbonyl[13–16] and dinitrogen[13] complexes, the ferrocyanide[17] and ferricyanide[18] ions, the iron(II) pentacyanides,[19] dioxygen complexes,[10] etc. However, very few calculations have been performed for transition-metal complexes with phosphorus ligands.[10,11] In the present paper we shall report MS–Xα calculations for tetrakis(trifluorophosphine)nickel, $Ni(PF_3)_4$. As in previous papers[13] the main interest will be on the wave function for the ground state and what it reveals in terms of the bonding mechanisms. Preliminary calculations carried out on model systems of the type L–Ni–PH_3 (L = CO, N_2) have shown that some Ni → P π back-donation exists. However, the P 3p rather than the P 3d orbital seems to be involved.[11] Another interesting result was that the P 3p occupancy depends on the cone angle (for a definition of this parameter see, for instance ref 7 and references therein).

In order to analyze the participation of the P 3d orbital in the Ni–P bond, two MS–Xα calculations on $Ni(PF_3)_4$, one with d-type partial waves on the P atom (*l* up to 2 in the P atomic sphere) and one with only s- and p-type partial waves (*l* up to 1), have been performed. Very different results are obtained for the total Ni 3d → P π-back-donated charge. The use of d-type functions drastically increases the π-acceptor capability of the P atom and, as a consequence, the Ni–P π bonding. The analysis of the P 3p and 3d components for each MO in the e and t_2 symmetries reveals that after the inclusion of the P 3d function the acceptor capability of the P 3p orbital is considerably increased. On the other hand, there is not a proper 3d acceptor orbital on the P atom. A possible mechanism for the interaction of a metal $3d_\pi$ system with the P 3p orbital, analogous to the hyperconjugation mechanism, will be discussed. At the same time, the possibly way in which the 3d function on the P atom can influence the π-acceptor properties of the 3p orbital will be analyzed in detail.

Computational Details

The MS method[12] with Slater's local Xα exchange has been applied to the $Ni(PF_3)_4$ molecule. For the Ni–P and P–F distances the values obtained from electron diffraction were used.[20] The values of the Slater

---

(3) Cotton, F. A. *Inorg. Chem.* **1964**, *3*, 702–711. Graham, W. A. G. *Ibid.* **1968**, *7*, 315–321.

(4) Green, J. C.; King, D. I.; Eland, J. H. D. *J. Chem. Soc. D* **1970**, 1121–1122. Hillier, H. I.; Saunders, V. R.; Ware, M. J.; Bassett, P. J.; Lloyd, D. R.; Lynaugh, N. *Ibid.* **1970**, 1316–1317.

(5) Yarbrough, L. W.; Hall, M. B. *Inorg. Chem.* **1978**, *17*, 2269–2275.

(6) Corderman, R. R.; Beauchamp, J. L. *Inorg. Chem.* **1977**, *16*, 3135–3139.

(7) Cotton, F. A.; Wilkinson, G. "Advanced Inorganic Chemistry", 4th ed.; Interscience: New York, 1980; pp 87–90.

(8) Xiao, S. X.; Trogler, W. C.; Ellis, D. E.; Berkovitch-Yellin, Z. *J. Am. Chem. Soc.* **1983**, *105*, 7033–7037.

(9) Braga, M., to be submitted for publication.

(10) Norman, J. G. *J. Am. Chem. Soc.* **1974**, *96*, 3327–3328.

(11) Larsson, S.; Braga, M.; de Mello, P. C.; Hehenberger, M.; Tang-Kai, A., paper presented at the First EUCHEM Conference on the Electronic Structure of Transition Metal Complexes, Maynooth, Ireland, 1978.

(12) Johnson, K. H. *J. Chem. Phys.* **1966**, *45*, 3085–3095; *Adv. Quantum Chem.* **1973**, *7*, 143–185.

(13) Braga, M.; Larsson, S.; Leite, J. R. *J. Am. Chem. Soc.* **1979**, *101*, 3867–3873. Larsson, S.; Braga, M. *Int. J. Quantum Chem.* **1979**, *15*, 1–5.

(14) Johnson, J. B.; Klemperer, W. G. *J. Am. Chem. Soc.* **1977**, *99*, 7132–7137. Bursten, B. E.; Freier, D. G.; Fenske, R. F. *Inorg. Chem.* **1980**, *19*, 1810–1811.

(15) Howard, I. H.; Pratt, G. W.; Johnson, K. H.; Dresselhauss, G. *J. Chem. Phys.* **1981**, *74*, 3415–3419.

(16) McIntosh, D. F.; Ozin, G. A.; Messmer, R. P. *Inorg. Chem.* **1981**, *20*, 3640–3650.

(17) Guenzburger, D.; Maffeo, B.; de Siqueira, M. L. *J. Phys. Chem. Solids* **1977**, *38*, 35–39.

(18) Guenzburger, D.; Maffeo, B.; Larsson, S. *Int. J. Quantum Chem.* **1977**, *12*, 383–396.

(19) Braga, M.; Pavão, A. C.; Leite, J. R. *Phys. Rev. B: Condens. Matter* **1981**, *23*, 4328–4336.

Table II. Comparison of the MO Energies and the Experimental Ionization Potentials for $Ni(PF_3)_4$[b]

orbital	orbital energy, eV	ionization potential,[a] eV	nature of the orbital
$17t_2$	0.0	0.0	Ni 3d
7e	1.01	1.03	Ni 3d
$16t_2$	3.53	3.54	PF_3 $8a_1$ (lone pair)
$11a_1$	3.99		
$1a_2$	5.65	...	PF_3 $1a_2$
$7t_1$	5.72		
$6t_1$	6.07		
6e	6.15	6.28	PF_3 6e
$15t_2$	6.19		
$14t_2$	6.66		
$5t_1$	6.78	7.88	PF_3 5e
5e	6.79		
$13t_2$	7.21		
$10a_1$	7.91	...	PF_3 $7a_1$
$12t_2$	9.27		
4e	9.81	9.72	PF_3 4e
$4t_1$	9.83		

[a] Reference 4a. [b] Both the calculated and the experimental values are referred to the energy of the HOMO level, $17t_2$.

exchange parameter α were taken from Schwarz.[21] A weighted average of the atomic values was used in the outer-sphere and intersphere regions. A regular T_d symmetry was assumed for the molecule, and the PF_3 groups were kept fixed; i.e., no rotation around the C_3 axis or changes in the cone angle were allowed. In order to reduce the charge in the intersphere region and to get convergence in the SCF procedure, a partitioning of the molecular space using overlapping spheres was adopted. For the P and F we used the same radii as in ref 22 ($r_P = 2.1382$ au, $r_F = 1.7358$ au). To obtain a better description of the metal 3d levels in accordance with our previous experience on MS calculations,[19] a small radius for the Ni atomic sphere was used ($r_{Ni} = 2.25$ au). With the present model only a small fraction of the total electronic charge lies in the intersphere region and the charge outside the molecular space (outer region) is completely negligible. The energy spectrum is also in good agreement with the experimental photoelectron spectrum (see next section). In particular, the calculated d–d splitting ($17t_2$–7e splitting) is 1.01 eV, which compares extremely well with the experimental value of 1.03 eV.[4]

Ni–P Bonding

The calculated energy spectra for $Ni(PF_3)_4$ with d-type partial waves on P (l up to 2) and with only s- and p-type partial waves (l up to 1) are given in Figure 1. The corresponding orbital energies, charge distributions, and orbital characters are presented in Table I. We have included only the $Ni(PF_3)_4$ MO's arising from the PF_3 6–$9a_1$, 4–6e, and $1a_2$ MO's, i.e. P 3s and 3p and F 2p levels and the Ni 3d orbital. The $9a_1$–$11t_2$, $10a_1$–$13t_2$, and $11a_1$–$16t_2$ pairs correspond to the PF_3 $6a_1$, $7a_1$, and $8a_1$ orbitals, respectively, with different degrees of Ni 4s (mainly in the $8a_1$ level) and Ni 3d, 4p ($16t_2$) admixture. The remaining levels, $1a_2$, 4–6e, 4–$6t_1$, and $12t_2$, $14t_2$, and $15t_2$ are PF_3 4e, 5e, 6e, and $1a_2$. The highest occupied MO and the orbital immediately below, $17t_2$ and 7e, respectively, are the crystal field Ni 3d levels with a large ligand contribution mainly in the $17t_2$ level. The lowest unoccupied MO, $18t_2$, corresponds to the PF_3 7e (π^*) orbital and also has a large Ni 3d component.

The ordering of the energy levels is completely similar for the two calculations performed, i.e. with and without 3d functions on the P atom. However, there are differences in the composition of some orbitals which clearly indicate a weakened metal–ligand interaction when the P 3d function is not included. Additional evidence is provided by the d–d splitting: 0.86 eV for the calculation without d functions on the P atom against the 1.01 eV corresponding to the calculation with d functions.

Table III. π-Back-Donated Charge

$Ni(PF_3)_4$ (l up to 2 on P)	1.23 (t_2, 0.92; e, 0.31)
$Ni(PF_3)_4$ (l up to 1 on P)	0.76 (t_2, 0.62; e, 0.14)
$Ni(CO)_4$[a]	1.53
$Ni(N_2)_4$[a]	1.18

[a] Reference 13.

Table IV. Electron Population of Valence Orbitals for the Ni Atom in $Ni(PF_3)_4$ (l up to 2 on P)

	electron population		
orbital	4s	4p	3d
$8a_1$	0.00		
$9a_1$	0.05		
$10a_1$	0.18		
$11a_1$	0.82		
4e			0.00
5e			0.00
6e			0.01
7e			3.68
8e			0.31
$11t_2$		0.07	0.01
$12t_2$		0.01	0.04
$13t_2$		0.19	0.04
$14t_2$		0.00	0.02
$15t_2$		0.02	0.00
$16t_2$		1.04	1.49
$17t_2$		0.98	3.49
$18t_2$		...	0.79
$19t_2$		...	0.13

total charge: 3s, 1.99; 3p, 5.98; 3d, 8.77; 4s, 1.05; 4p, 2.31

We have performed ground-state calculations, and we cannot expect a quantitative agreement between our calculated energy spectrum and the experimental photoelectron spectrum; i.e., our energies cannot be considered as ionization energies. However, as we can see in Table II, the ordering of the energy levels is quantitatively correct and the calculated energy separation among the different groups of levels originating from a given Ni or PF_3 level is also in good agreement with the experimental values; i.e., the main features of the $Ni(PF_3)_4$ electronic structure are adequately described by the present MS calculations.

In analogy with other π-acceptor ligands, the bonding between a transition-metal atom and trivalent phosphorus compounds may be described as taking place through σ donation from the highest occupied MO of a_1 symmetry ($8a_1$ in PF_3), which is a "lone pair" orbital largely localized on the P atom, and by electron transfer from the metal 3d levels into the first virtual MO of e symmetry (7e π^* in PF_3). It is commonly thought[7] that this level is also largely localized on the P atom with a substantial 3d character.

The Ni atom in $Ni(PF_3)_4$ has a closed-shell $3d^{10}$ configuration, and therefore it is not possible to have σ donation to the Ni 3d shell.[13,23] However, σ donation to the Ni 4s and 4p orbital can occur and it is actually found to be very large (see below). In the case of the 4p orbital there is also an important Ni 3d → 4p transfer which for symmetry reasons is impossible to evaluate separately from the σ contribution.

In order to calculate the Ni 3d → P π back-donation, we have used the method developed in ref 13. The total π-back-donated charge for $Ni(PF_3)_4$ (with and without d-type partial waves on the P atom) is given in Table III. For comparison purposes the corresponding values for $Ni(CO)_4$ and $Ni(N_2)_4$ were also included. The Ni 3d population for valence orbitals of e and t_2 symmetry is shown in Table IV.

We cannot expect that the calculated value of the π-back-donated charge is quantitatively correct. There are different sources

---

(20) Almenningen, A.; Andersen, B.; Astrup, E. E. *Acta Chem. Scand.* **1970**, *24*, 1579–1584.

(21) Schwarz, K. *Phys. Rev. B: Solid State* **1972**, *5*, 2466–2468.

(22) Weber, J.; Geoffroy, M. *Theor. Chim. Acta* **1977**, *43*, 299–306.

(23) Kitaura, K.; Sakaki, S.; Morokuma, K. *Inorg. Chem.* **1981**, *20*, 2292–2297. Sakaki, S.; Kitaura, K.; Morokuma, K. *Ibid.* **1982**, *21*, 760–765. Sakaki, S.; Kitaura, K.; Morokuma, K.; Ohkubo, K. *Ibid.* **1983**, *22*, 104–108.

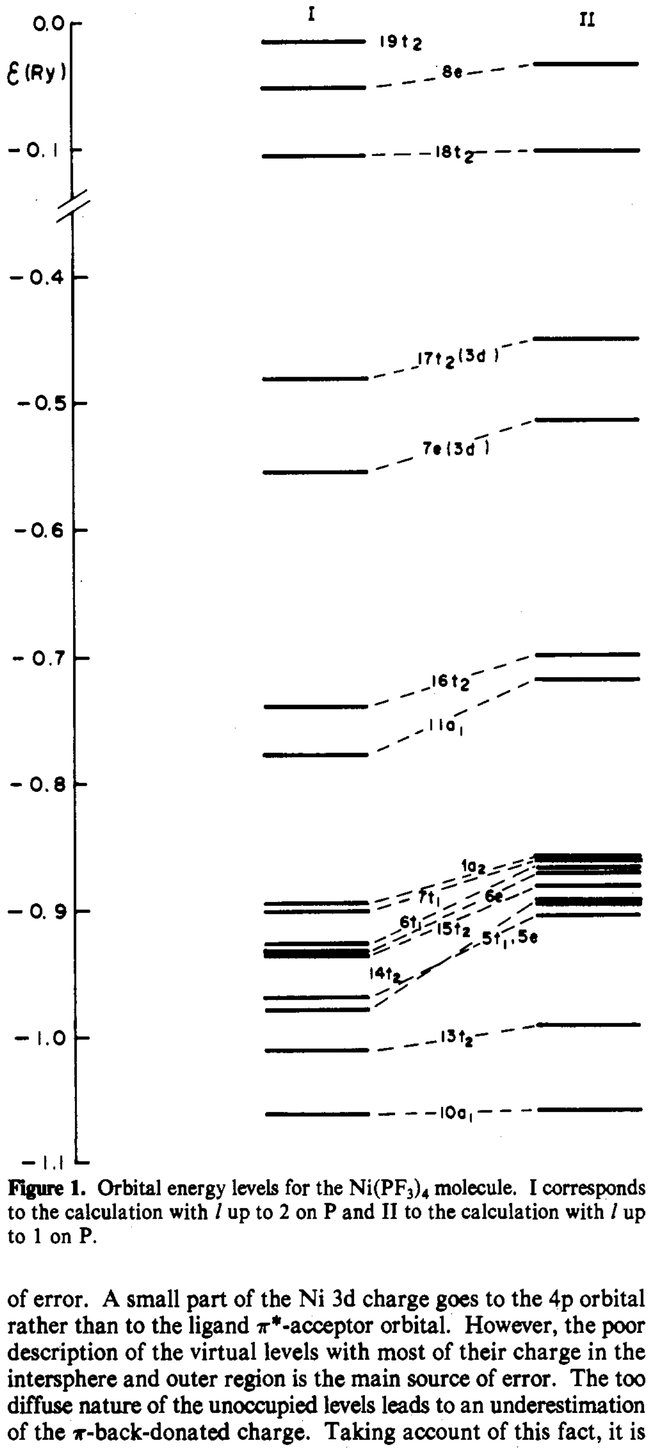

Figure 1. Orbital energy levels for the $Ni(PF_3)_4$ molecule. I corresponds to the calculation with l up to 2 on P and II to the calculation with l up to 1 on P.

of error. A small part of the Ni 3d charge goes to the 4p orbital rather than to the ligand π^*-acceptor orbital. However, the poor description of the virtual levels with most of their charge in the intersphere and outer region is the main source of error. The too diffuse nature of the unoccupied levels leads to an underestimation of the π-back-donated charge. Taking account of this fact, it is then possible to conclude that the π back-donation is of about the same magnitude for the nickel carbonyl and trifluorophosphine complexes.

The Ni 4s and 4p orbitals are very diffuse, and they are largely localized in the ligand region. In the same way as described in ref 13 we can evaluate the occupancies for both orbitals. These values are included in Table IV. The total 4s and 4p charges are smaller than the corresponding values for $Ni(CO)_4$.[13] In particular, the 4p occupancy is lower than the value corresponding to a sp^3 hybridization. However, in analogy with the $Ni(CO)_4$, the highest MO for PF_3 ($8a_1$) is involved in the 4s, 4p bonding. Since this orbital does not have strong bonding character, it is not likely that the 4s,4p contribution changes the strength of the PF_3 bond to any significant extent.

Structure of the π^* Acceptor Orbital. Both SCF–Xα[8] and ab initio[9] calculations clearly indicate that the first unoccupied level of π type in PF_3 is largely localized on the P atom and that is has essentially P 3p character with a low P 3d component. The same conclusion is true for PH_3,[8,9] $P(CH_3)_3$,[8] and PCl_3.[9] By inspection of the coefficients in the corresponding MS wave function we find that the lowest unoccupied MO in $Ni(PF_3)_4$, $18t_2$, corresponds to the PF_3 7e π^* orbital, i.e., it is substantially P 3p in character. Due to the diffuse nature of this level (almost 60% of its charge density is lying in the intersphere and outer region) it is very difficult to estimate quantitatively the extent of the P 3p and 3d components. A rough estimate gives ~40% of P 3p character and ~10–15% of P 3d. A similar description also applies to the first unoccupied level in e symmetry, 8e. It is then clear that the π-back-donation charge is going into the P 3p orbital.

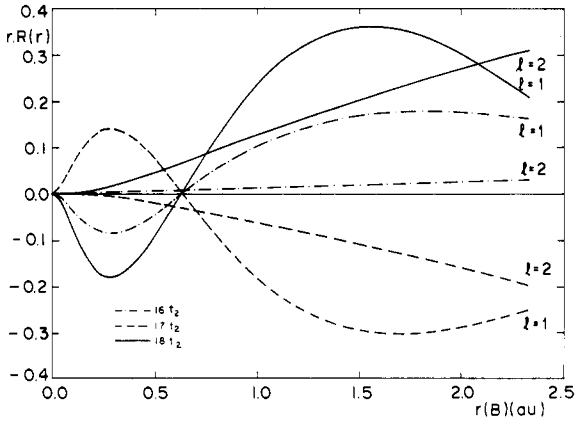

Figure 2. l = 1 and l = 2 components in the P sphere for the two highest occupied MO's and the lowest unoccupied MO of t_2 symmetry ($16t_2$, $17t_2$, and $18t_2$, respectively) for $Ni(PF_3)_4$ (calculation with l up to 2 on P).

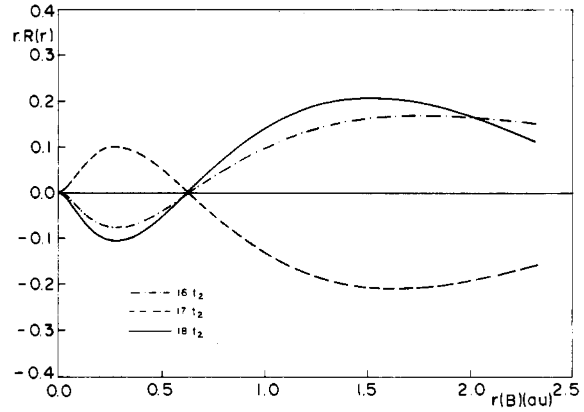

Figure 3. l = 1 component in the P sphere for the same orbitals as in Figure 2 for $Ni(PF_3)_4$ (calculation with l up to 1 on P).

The analysis of the l = 1 and l = 2 components in the P atomic region for both calculations, i.e. with and without d partial waves on P, will allow us to understand the role of the P 3d orbitals in the back-donation process. In Figure 2 give the l = 1 and l = 2 components in the P atomic region for three valence orbitals: the two highest occupied MO's $16t_2$ and $17t_2$ and the first unoccupied MO $18t_2$. In Figure 3 we have plotted the l = 1 component in the P atomic region for the same valence orbitals and for the calculation using only s- and p-type functions on P. We can see that the P 3p component is considerably larger when d-type functions are used on the P atom. It appears that the role of the P 3d orbital is chiefly to increase the π-acceptor capability of the P 3p orbital rather than to accept charge from the transition metal. On the other hand, the l = 2 component on P can be regarded as the tail of the atomic orbitals on Ni and F. The P 3d orbital is very diffuse and should therefore be mainly lying in the Ni and F atomic regions.

The enhancement of the P 3p participation in the Ni–P bond by the P 3d orbitals can be understood in two different ways. The 3d functions centered on the P atom can mix with the 3p functions.[8-10] This mixing gives a p–d hybrid orbital more efficiently directed toward the metal atom, and in this way the Ni 3d–P 3p overlap is considerably improved. On the other hand, the P 3d functions also contribute to the P–F bond, and the net result of this contribution is to facilitate the shift of electronic charge toward the F atoms.[9] This withdrawal of charge from the P atom mainly empties the 3p valence level and results in a π^* empty orbital with larger 3p character, which is as a consequence more suited to accept charge from the metal atom.[9] Both mechanisms lead to exactly the same result, i.e. the 3p participation being enhanced via the 3d orbitals, and it seems likely that they are contributing together to strengthen the Ni–P bond.

Hyperconjugation in the Ni–P Bonding. Hyperconjugation is a concept widely used in organic chemistry and in its classical form consists in the interaction of a π-type orbital with an empty p orbital, causing a lowering in energy.[24] This interaction can explain why a CH_3 group can stabilize a carbonium ion, etc. The substitution of the H atoms in the CH_3 group by a more electronegative element like F results in a CF_3 group, which in turn can stabilize an anion. However, this process will involve both the π (occupied) and the π^* (empty) orbitals of the CF_3 group. In CF_3, the π orbital has a small C 2p component and the π^* orbital a large C 2p character. The π^* orbital thus becomes more available for electron acceptance and can easily interact with an atom or radical with an excess of charge.

The valence electronic configuration of a CH_3^- group closely resembles that of the PH_3 molecule. The same is also valid for CF_3^- and PF_3. In PF_3 the pair of π orbitals that can interact with the π system of an anion are 4e (π) and the 7e (π^*). The P 3p component in 4e is very small while the 7e is largely a P 3p orbital with a small P 3d participation (see above). The interaction of a PF_3 molecule with a transition metal in a low oxidation state (an "anion") and the acceptance of charge into the P 3p orbital via the 7e π^* level may be considered as a kind of hyperconjugation process essentially analogous to the hyperconjugation in organic compounds.

Registry No. $Ni(PF_3)_4$, 13859-65-9; Ni, 7440-02-0; P, 7723-14-0.

---

[24] Fleming, I. "Frontier Orbitals and Organic Chemical Reactions"; Wiley: New York, 1978; pp 80–85.

Contribution from the Department of Chemistry,
North-Eastern Hill University, Shillong 793003, India

First Synthesis and Structural Assessment of Alkali-Metal Triperoxovanadates(V), $A[V(O_2)_3]$

Mihir K. Chaudhuri,* Soumitra K. Ghosh,
and Nashreen S. Islam

Received December 28, 1984

It is probably owing to biochemical significance,[1,2] and importance in the oxidation chemistry,[3] of peroxo–transition-metal compounds that the study on peroxovanadium chemistry has emerged as one of the active areas of research.[4-10] The vanadium–hydrogen peroxide system is complicated owing to the formation of peroxovanadates of varied compositions and colors with varying acidity or alkalinity of the reaction media.[7,11,12] The blue tetraperoxovanadate(V) $K_3[V(O_2)_4]$ has been known,[13] presumably having a structure analogous to that of $K_3[Cr(O_2)_4]$.[14] However, the triperoxovanadates(V) $A[V(O_2)_3]$ (A = alkali metal) have not been synthesized and isolated in the solid state although the hetero triperoxovanadates(V) $A_2[V(O_2)_3X]$ (X = F or Cl) have been reported recently.[15] In view of this it was thought that the successful synthesis and isolation of the blue $[V(O_2)_3]^-$ complex would provide some fundamental information concerning the minimum number of O_2^{2-} ligands, per V^{5+} center, required for the formation of a blue peroxovanadate(V) species. The present paper reports the synthesis, isolation in the solid state, and characterization of the blue alkali-metal triperoxovanadates(V) $A[V(O_2)_3]$ (A = Na or K).

Experimental Section

The chemicals used were all reagent grade (B.D.H., E. Merck) products. Infrared spectra were recorded on a Perkin-elmer Model 983 spectrophotometer. The laser Raman spectra were recorded on a SPEX Ramalog Model 1403 spectrometer. The 6328-Å Laser line from a helium–neon laser was used as the excitation source. The scattered light at 90° was detected with the help of a cooled RCA 31034 photomultiplier tube and a photon-counting processing system. The spectra were recorded at ambient temperatures by making freshly prepared solutions of the samples or pressed pellets of the compounds. Molar conductance measurements were made with a Philips PR 9500 conductivity bridge. Magnetic susceptibilities were measured by the Gouy method using $Hg[Co(NCS)_4]$ as the standard. The UV–vis spectra were recorded on a Beckman Model UV-26 spectrophotometer.

Synthesis of Alkali-Metal Triperoxovanadates(V), $A[V(O_2)_3]$ (A = Na or K). Recommended Procedure. To finely powdered V_2O_5 was added an excess of 30% hydrogen peroxide, with slow stirring, in the molar ratio of V_2O_5:H_2O_2 as 1:42.5. Solid alkali-metal hydroxide, AOH, was slowly added to the above mixture under continuous stirring, until a blue color was developed (molar ratio V_2O_5:H_2O_2:AOH as 1:42.5:(10–12)). The blue solution was then cooled in an ice-water bath for ca. 30 min, followed by the addition of an excess of precooled ethyl alcohol until the blue microcrystalline $A[V(O_2)_3]$ ceased to appear. The blue compound was separated by centrifugation, washed four or five times with cold ethanol, and finally dried in vacuo over phosphorus pentoxide. The reaction was monitored by IR spectroscopy. The complete disappearance of the sharp band at ca. 950 cm^{-1} due to $\nu_{\mathrm{V=O}}$, in the product isolated from a small amount of the blue solution, indicates completion of the reaction.

The yield of $Na[V(O_2)_3]$ was 0.8 g (86%) obtained from the reaction of 0.5 g (2.7 mmol) of V_2O_5 with 13 cm^3 (114.6 mmol) of 30% H_2O_2 and 1.1 g (27.5 mmol) of NaOH, while that of $K[V(O_2)_3]$ was 0.9 g (90%) obtained from 0.5 g of V_2O_5 with 13 cm^3 of 30% H_2O_2 and 1.8 g (32 mmol) of KOH.

Elemental Analyses. Vanadium was determined volumetrically by redox titration with potassium permanganate.[15,16] The estimation of total peroxide content, in each compound, was accomplished by redox titrations with a standard cerium(IV) solution[17] and also separately with a standard potassium permanganate solution.[18] In a representative titrimetric procedure for the estimation of total amount of coordinated peroxide, a weighed amount of the sample under investigation was added to 100 cm^3 of cold distilled water, acidified with 2 cm^3 of concentrated sulfuric acid, containing ca. 1.5 g of boric acid. The whole was gently stirred on a magnetic stirrer and titrated with a standard potassium permanganate solution[17] or with a standard Ce^{4+} solution.[18] Sodium and potassium were determined by the methods described in our earlier paper.[15]

The results of elemental analyses, molar conductance values, IR and laser Raman band positions and their assignments are summarized in Table I.

---

[1] Guilard, R.; Latour, J.; Lecompte, C.; Marchon, J. *Inorg. Chem.* **1978**, *17*, 1228.

[2] Djordgevic, C. *Chem. Br.* **1982**, *18*, 554.

[3] Bortolini, O.; Furia, F. D.; Modena, G. *J. Am. Chem. Soc.* **1981**, *103*, 3924.

[4] Vuletic, N.; Djordgevic, C. *J. Chem. Soc.* **1973**, 1137.

[5] Yamada, S.; Ukei, Y.; Tanaka, H. *Inorg. Chem.* **1976**, *15*, 964.

[6] Funahashi, S.; Harraguchi, K.; Tanaka, M. *Inorg. Chem.* **1977**, *16*, 1349.

[7] Wieghardt, K. *Inorg. Chem.* **1978**, *17*, 57.

[8] Quilitzsch, U.; Wieghardt, K. *Inorg. Chem.* **1979**, *18*, 869.

[9] Funahashi, S.; Ishihara, K.; Tanaka, M. *Inorg. Chem.* **1981**, *20*, 51.

[10] Mitra, R.; McAndrew, T. P.; Mitra, G. *J. Inorg. Nucl. Chem.* **1981**, *43*, 421.

[11] Dean, G. A. *Can. J. Chem.* **1961**, *39*, 1174.

[12] Connor, J. A.; Ebsworth, E. A. V. *Adv. Inorg. Chem. Radiochem.* **1964**, *6*, 292.

[13] Clark, R. J. H.; Brown, D. "The Chemistry of Vanadium, Niobium and Tantalum"; Pergamon Press: Elmsford, NY, 1975; Pergamon Texts in Inorganic Chemistry Vol. 20, p 519.

[14] Swalen, J. D.; Ibers, J. A. *J. Chem. Phys.* **1962**, *37*, 17.

[15] Chaudhuri, M. K.; Ghosh, S. K. *Inorg. Chem.* **1982**, *21*, 4020; **1984**, *23*, 534.

[16] Steele, M. C.; Hall, F. M. *Anal. Chim. Acta* **1953**, *9*, 384.

[17] Vogel, A. I. "A Text Book of Quantitative Inorganic Analysis"; Longmans, Green and Co.: New York, 1962; p 325.

[18] Vogel, A. I. "A Text Book of Quantitative Inorganic Analysis"; Longmans, Green and Co.: New York, 1962; p 295.

0020-1669/85/1324-2706$01.50/0 © 1985 American Chemical Society